

Kinetics of Austenite Recrystallization during the Annealing of Cold-rolled Fe-Mn-Al-C Steel

M. A. Sohrabizadeh, Y. Mazaheri* and M. Sheikhi

Department of Materials Engineering, Bu-Ali Sina University, Hamedan, Iran

ARTICLE INFO

Article history:

Received 3 December 2019

Revised 25 January 2020

Accepted 5 February 2020

Keywords:

Fe-Mn-Al-C steel

Recrystallization kinetics

JMAK model

ABSTRACT

In the current study, the recrystallization behavior of 75% cold-rolled Fe-22Mn-10Al-1.4C steel during annealing at 750, 770, 790, 810, and 830°C was studied. X-ray diffraction patterns and optical microscopy were used to characterize microstructures. The Vickers Micro-hardness test was used to characterize recrystallization kinetics during annealing. Johnson-Mehl-Avrami-Kolmogorov (JMAK) model was used to evaluate the experimental data. The as-homogenized microstructure illustrated only austenite with a high fraction of annealing twins, and austenite to martensite phase transformation was not observed after quenching at a high temperature and also until high thickness reduction. Avrami exponent was decreased from 0.76 to 0.42, with increasing the annealing temperature from 750 to 830°C. The activation energy value was determined to be ~175 kJ/mol, which was slightly higher than the diffusion activation energy of carbon in austenite.

© Shiraz University, Shiraz, Iran, 2020

1. Introduction

Lightweight steel alloys, based on the Fe-Mn-Al-C alloying system, have shown an excellent combination of strength and ductility due to the high values of manganese and aluminum, and have a wide range of industrial application predictions, such as automotive body applications, owing to their low-density and low price of manufacturing. Density reduction of up to 17% [1], tensile strength of higher than 1.2 GPa [2], ductility of about 77% [3], are some of their unique properties that prepare them for the cryogenic system [4], oxidation resistance in high temperatures [5], and impact-resistant [6] industrial applications. According to the stacking fault energy (SFE), the transformation induced plasticity

(TRIP) [7], twinning induced plasticity (TWIP) [8], and microband induced plasticity (MBIP) [9] are the best deformation mechanisms, for their low, medium, and high values of the SFE, respectively.

Much of the literature review focus on the texture and mechanical properties of Fe-Mn-Al-C alloys, and only a few essays are associated with the recrystallization kinetics of cold-rolled lightweight steels during the annealing at high temperatures [10-12]. Recrystallization is primarily controlling the nucleation and growth of free strain grains. Meanwhile, recrystallization kinetics is defined by the Johnson-Mehl-Avrami-Kolmogorov (JMAK) model, which characterizes the recrystallization and phase transformations, that has been shown in Eq. (1):

* Corresponding author

E-mail address: y.mazaheri@basu.ac.ir (Y. Mazaheri)

$$X_{\text{rec}} = 1 - \exp(-kt^n) \quad (1)$$

Where X_{rec} is phase volume recrystallized fraction, t is annealing time, k is a temperature-dependent rate constant, and n is the Avrami exponent.

The theoretical value of n is considered 4 if the nucleation rate is constant, while all nuclei are formed at the initial stage of the annealing process. In most metal transformations, induced by diffusion, the Avrami exponent is considered ranging from 0.5 to 2.5 [12]. Lu et al. [10] showed that, in Fe-Mn-C alloy, depending on the annealing temperature, n value changed from 0.7 at 560°C to 1.3 at 700°C. Torabinejad et al. [13] have probed the effect of annealing temperature on the austenite grain boundary migration rate and showed that, by increasing annealing temperature, the grain boundary migration rate decreased at the early stage of recrystallization.

However, the recrystallization of austenite at the early stage of annealing time and various temperatures differs from previous studies. Nevertheless, the present study aims at clarifying the recrystallization kinetics of Fe-Mn-Al-C alloy during different annealing times, and temperatures, carried out by the JMAK model.

2. Experimental Procedure

2.1. Material and processing

The chemical composition of the lightweight steel, in the current study, is presented in Table 1. The alloy was made from high purity iron, manganese, aluminum, and carbon by inducing melting in an argon atmosphere. The schematic of the thermomechanical process applied to the investigated alloy is shown in Fig. 1. After casting, the ingot was homogenized at 1200°C for 120 min, and water quenched, subsequently. Samples were cold-rolled up to a thickness reduction of 75%. To investigate the recrystallization kinetics, under different annealing conditions, samples were heated at 750, 770, 790, 810 and 830°C for 30, 60, 120, 240, 360, 600, 1200, 1800, 3600 s in a furnace, and were cooled in the water.

Table 1. Chemical composition of the investigated steel

Element	Mn	Al	C
(wt.%)	22	10	1.4

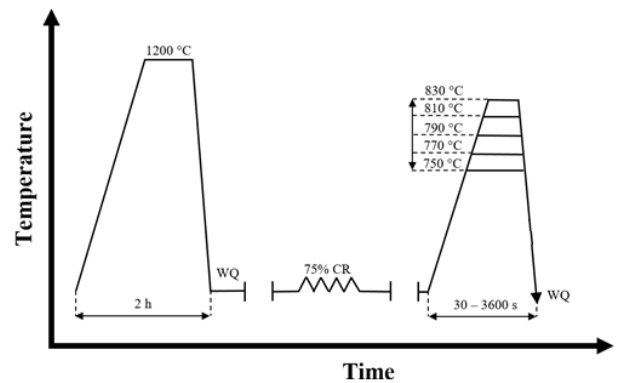


Fig. 1. The schematic of the thermomechanical process applied to the investigated alloy.

2.2. Analysis techniques

The surface morphologies of the samples, according to the conventional metallographic preparation, and etched with 5-10% nital solution, were analyzed by optical microscopy (OM). The X-ray diffraction characterization was carried out by using Cu α radiation ($\lambda = 0.15406$ nm) generated at 40 kV and 30 mA, with scanning step of 0.01 degree and time per step of 1 s. The phase volume fractions were determined by XRD patterns. Commonly, Rietveld refinement is used for quantitative phase analysis. In a texture strain-free sample, the intensity of the phase peak is divided by material scattering factor R_{hkl} and it is compared with that of the standard phase peak. In the current study, MAUD software has been used for quantitative phase fraction determination. The microhardness of annealed samples was investigated by using a Vickers hardness test machine, under a load of 300 g for 15 s, representing an average of 3 indentations.

3. Results and Discussion

3.1. Microstructure

The optical micrograph of Fe-22Mn-9Al-1.4C, after homogenizing, is shown in Fig. 2(a). As can be seen, the as-homogenized microstructure contained a full austenite matrix. During the homogenized annealing, a high fraction of annealing twins (yellow arrows) was revealed in some austenite grains.

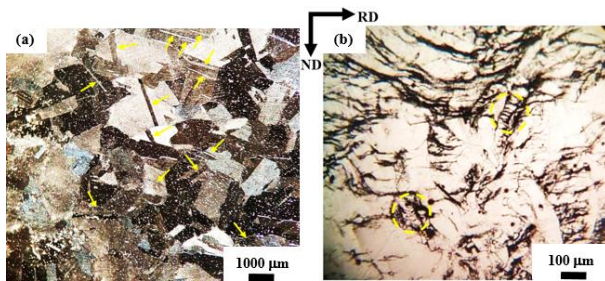


Fig. 2. Optical micrograph after (a) homogenizing and (b) cold-rolling.

The average grain size of austenite was determined by about 1112 μm . The microstructure of cold-rolled samples contained lamellar structures (Fig. 2(b)). As is evident, some grains were recrystallized by the dynamic recrystallization (DRX) phenomenon (dotted yellow circles). The occurrence of DRX during high-temperature deformation, which is known as geometric DRX, has been recognized for some time. However, recent research has shown that severe cold-working of a metal can also result in a microstructure which consists almost entirely of high-angle grain boundaries, and may undergo continuous DRX (CDRX). Therefore, CDRX of metals deformed at ambient temperatures is considered as the possible mechanism in the formation of such microstructures [14].

The progress of the annealing process is shown in

Fig. 3. At the first moment of the annealing process, on the cold-rolled samples, grain nucleations were generated immediately, on such high energy places as grain boundaries or shear bands. By increasing annealing time, some of the elongated grains parallel to the rolling direction, were replaced by equiaxed recrystallized grains with distinct boundaries. As it is clear, by increasing annealing time, the size of the recrystallized grains increased, consequently. X-ray diffraction patterns were used to provide phase transformation during homogenizing, cold-working, and recrystallization on the investigated alloy (Fig. 4). As can be seen, only austenite peaks were observed after homogenizing and cold working. The SFE of a current alloy was estimated by SFE maps [11] to be about 85 mj/m^2 . Due to the high value of the SFE of Fe-Mn-Al-C alloys, $\gamma \rightarrow \epsilon$ phase transformation did not occur during quenching at high temperatures and also until high thickness reduction. Tian et al. [15] showed that if SFE increases and passes 45 mj/m^2 , $\gamma \rightarrow \epsilon$ phase transformation does not occur. In the Fe-Mn-Al-C alloying system, austenite is not a stable phase, and any thermal treatment could lead to the decomposition of this phase [16]. The main cause of this phenomenon is related to the decreasing distance between partial dislocations and easy cross slip. By increasing SFE, the deformation mechanism changes the transformation induced plasticity (TRIP) to the twinning induced plasticity (TWIP), and finally, in high SFE values, the microband induced plasticity (MBIP) becomes the primary deformation mechanism [17]. Therefore, Austenite is decomposed after recrystallization at 770°C for 4 min, and ferrite appears. The ferrite volume fraction was determined by XRD patterns. The volume fraction of ferrite was about 10%, and it went up by increasing annealing time.

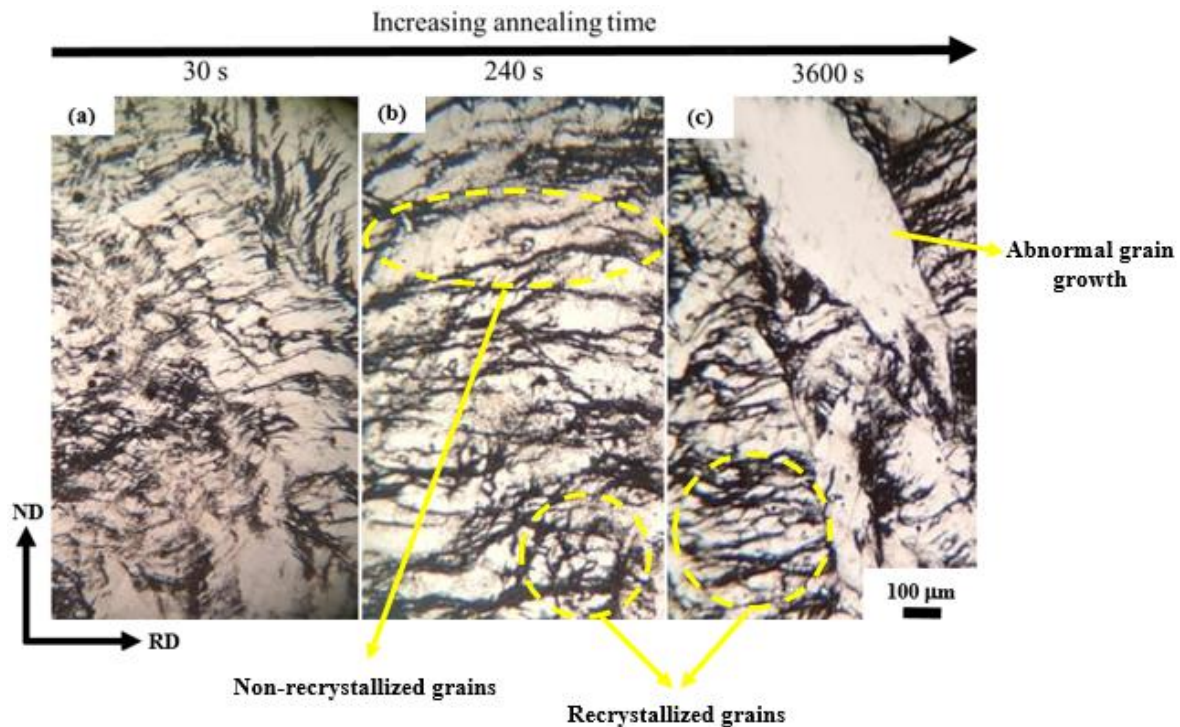


Fig. 3. Optical micrograph of recrystallized samples at 770°C for (a) 30, (b) 240 and (c) 3600 s.

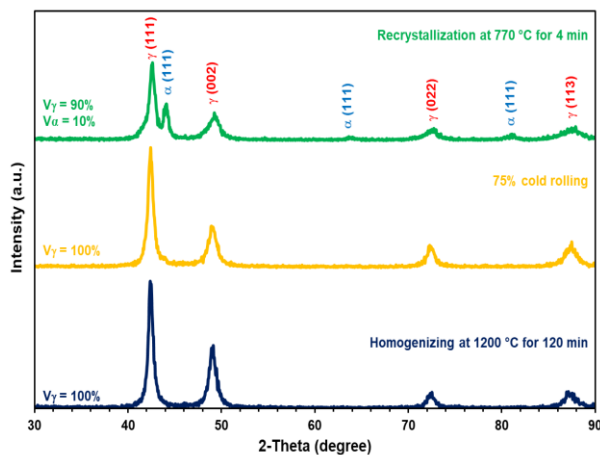


Fig. 4. X-ray diffraction patterns after homogenizing, cold-rolling, and recrystallizing.

3. 2. Recrystallization kinetics

Figure 5(a) illustrates the decrease of hardness vs. annealing time at different temperatures. After 120 s, hardness decreases significantly at all temperatures. By increasing annealing temperature, hardness decreases gradually. After 20 min of annealing, hardness shows a downward trend with a few changes. After that time,

recrystallization is complete; and hardness decreases due to grain growth. The recrystallized volume fraction vs. annealing time, at different temperatures, is exhibited in Fig. 5(b). As it is clear, a significant recrystallized volume fraction occurs before 30 s of annealing. It could be due to fast recrystallization behavior, especially at high annealing temperatures.

Considering the fact that austenite transformation is induced by diffusion, and only this phase recrystallizes before 30 s, the recrystallized volume fraction could be introduced by Eq. (2) [18]:

$$X_{\text{rec}} = (H_{\text{initial}} - H_{\text{time}}) / (H_{\text{initial}} - H_{\text{final}}) \quad (2)$$

Where H_{initial} , H_{time} , and H_{final} represent hardness after cold rolling, in a specific annealing time, and after full recrystallization, respectively. In order to characterize the kinetics of austenite recrystallization, the JMAK model was applied (Eq. (1)). The Avrami exponent n can be achieved from the slope of $\ln(\ln(1/(1-X_{\text{rec}})))$ vs. $\ln(t)$ (Fig. 6). It is clear that the plots were approximately linear, and the slopes of the lines went down by increasing annealing temperature.

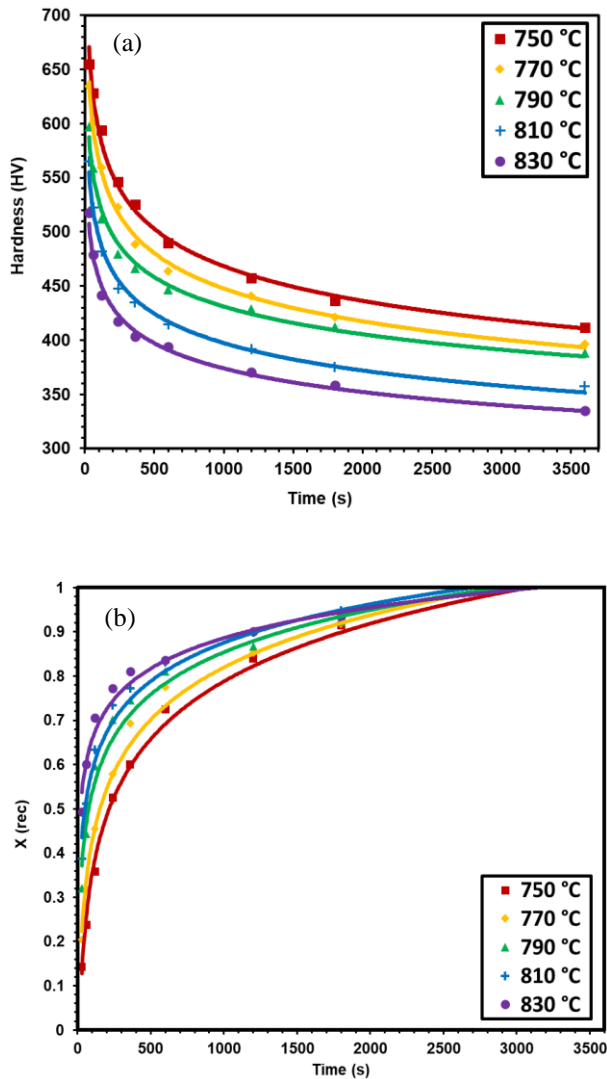


Fig. 5. (a) microhardness as a function of annealing time and (b) recrystallized volume fraction after 75% cold-rolling vs. annealing time.

Table 2 summarizes the value of the Avrami exponent at different temperatures. The theoretical value of the Avrami exponent for random nucleation is estimated from 0.67 to 1 [19]. The formation of austenite in dual-phase steel, studied by Mazaheri et al. [20] based on the intercritical annealing temperatures, showed that the Avrami exponent after 50 and 80% cold-rolling could change into 1.253 and 1.093, respectively. It should be noted that the nucleation of austenite, in the present study, was distributed entirely randomly, and it was controlled by diffusion.

Table 2. Avrami exponent values at different annealing temperatures

Annealing temperature (°C)	Avrami exponent
750	0.76
770	0.7
790	0.61
810	0.51
830	0.42

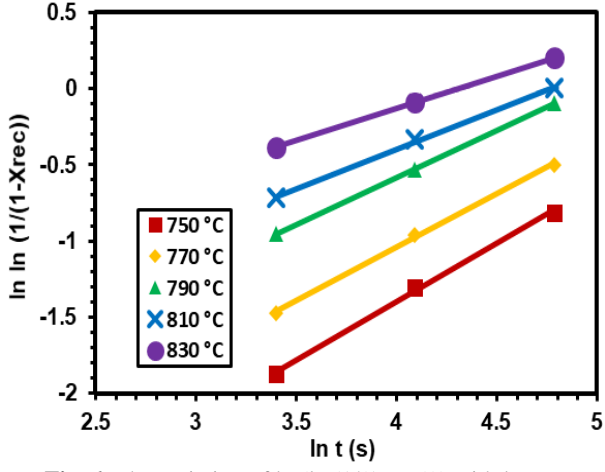


Fig. 6. The variation of ln (ln (1/(1-X_rec))) with ln t at different annealing temperatures.

As mentioned earlier, k-constant depends on temperature, and its value is obtained from Eq. (3):

$$\ln k = \ln A - (Q/RT) \tag{3}$$

Where A is the constant, Q is the activation energy, R is the universal gas constant (8.314 j/mol K), and T is temperature. By combining equations (1) and (3), the following equation is achieved:

$$\ln \ln (1/(1-X_{rec})) = \ln A + n \ln t - (Q/RT) \tag{4}$$

At constant annealing time, ln A + n ln t is a constant. Thus the plot of ln (ln (1/(1-X_rec))) vs. 1/T is roughly linear, and the Q value will be extracted from the slope of the curve. The experimental austenite formation kinetics after 75% cold working after 30 s of annealing is shown in Fig. 7. The activation energy value is estimated to be 175 kJ/mol, which is slightly higher than the diffusion activation energy of carbon in austenite (157 kJ/mol) [21]. This phenomenon could be attributed to the effects of alloying additions, such as manganese and aluminum.

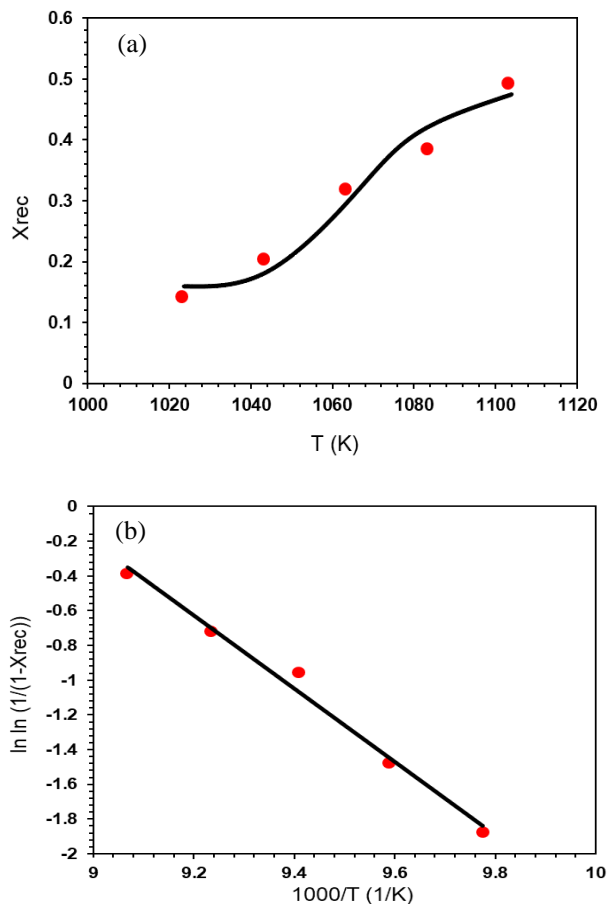


Fig. 7 The variation of (a) X_{rec} with T and (b) $\ln \ln (1/(1-X_{rec}))$ with $1/T$, after 75% cold-rolling and 30 s annealing.

4. Conclusions

The recrystallization kinetics in the 75% cold-rolled Fe-22Mn-10Al-1.4C alloy was investigated experimentally at temperatures ranging between 750 and 830°C. The effect of annealing time and temperature on the recrystallization kinetics constant values were studied. Based on the measurements the following conclusions can be made:

1. The microstructure after homogenizing showed only austenite with a high fraction of annealing twins. $\gamma \rightarrow \varepsilon$ phase transformation was not detected during quenching at high temperatures and also not until high thickness reduction.
2. After 120 s of annealing, hardness decreased significantly, and after 20 min, hardness did not change much due to the complete recrystallization and grain growth.

3. The kinetics of austenite recrystallization was characterized by the JMAK model showing the Avrami exponent to be 0.76 and 0.42 at 750 and 830 °C, respectively. The activation energy Q of the recrystallization was recorded ~ 175 kJ/mol that is slightly higher than the diffusion activation energy of carbon in austenite.

5. References

- [1] Y. P. Li, R. B. Song, E. D. Wen, F. Q. Yang, Hot deformation and dynamic recrystallization behavior of austenite-based low-density Fe-Mn-Al-C steel, *Acta Metallurgica Sinica* 29, no. 5 (2016) 441-449.
- [2] Y. Sutou, N. Kamiya, R. Umino, I. Ohnuma, K. Ishida, High-strength Fe-20Mn-Al-C-based Alloys with Low Density, *ISIJ International* 50, no. 6 (2010) 893-899.
- [3] S. S. Sohn, K. Choi, J. H. Kwak, N. J. Kim, S. Lee, Novel ferrite-austenite duplex lightweight steel with 77% ductility by transformation induced plasticity and twinning induced plasticity mechanisms, *Acta Materialia* 78 (2014) 181-189.
- [4] I. S. Kalashnikov, O. Acselrad, T. Kalichak, M. S. Khadyyev, L. C. Pereira, Behavior of Fe-Mn-Al-C steels during cyclic tests, *Journal of Materials Engineering and Performance* 9, no. 3 (2000) 334-337.
- [5] P. R. S. Jackson, G. R. Wallwork, High temperature oxidation of iron-manganese-aluminum based alloys, *Oxidation of Metals* 21, no. 3-4 (1984) 135-170.
- [6] K. T. Luo, P. W. Kao, D. Gan, Low temperature mechanical properties of Fe28Mn5Al11C alloy, *Materials Science and Engineering: A* 151, no. 1(1992) 15-18.
- [7] O. Gräßel, G. Frommeyer, C. Derder, H. Hofmann, Phase transformations and mechanical properties of Fe-Mn-Si-Al trip-steels, *Le Journal de Physique IV* 7, no. C5 (2007) 383-388.
- [8] M. M. Karkehabadi, A. Kermanpur, A. Najafzadeh, K. Kiani, Prediction of mechanical properties of twip steels using artificial neural network modeling, *International Journal of Iron & Steel Society of Iran* 15, no. 2 (2018) 27-37.
- [9] J. D. Yoo, K. T. Park, Microband-induced plasticity in a high Mn-Al-C light steel, *Materials Science and Engineering: A* 496, no. 1-2, (2008) 417-424.
- [10] Y. Lü, D. A. Molodov, G. Gottstein, Recrystallization

- kinetics and microstructure evolution during annealing of a cold-rolled Fe-Mn-C alloy, *Acta Materialia* 59, no. 8 (2011) 3229-3243.
- [11] O. A. Zambrano, Stacking fault energy maps of Fe-Mn-Al-C-Si steels: effect of temperature, grain size, and variations in compositions, *Journal of Engineering Materials and Technology* 138, no. 4 (2016).
- [12] J. Burke, *The kinetics of phase transformations in metals*, Pergamon Press INC., 1965.
- [13] V. Torabinejad, A. Zarei-Hanzaki, S. Moemeni, "An analysis to the kinetics of austenite recrystallization in Fe-30Mn-5Al steel, *Materials and Manufacturing Processes* 28, no. 1 (2012) 36-41.
- [14] A. Rollett, G. S. Rohrer, J. Humphreys, *Recrystallization and related annealing phenomena: third edition*, Elsevier, 2017.
- [15] X. Tian, R. Tian, X. Wei, Y. Zhang, "Effect of Al content on work hardening in austenitic Fe-Mn-Al-C alloys, *Canadian Metallurgical Quarterly* 43, no. 2 (2004) 183-192.
- [16] S. S. Sohn, H. Song, B-Ch Suh, J-H Kwak, B-J Lee, N. J. Kim, S. Lee, Novel ultra-high-strength (ferrite + austenite) duplex lightweight steels achieved by fine dislocation substructures (Taylor lattices), grain refinement, and partial recrystallization, *Acta Materialia* 96 (2015) 301-310.
- [17] S. Chen, R. Rana, A. Haldar, R. K. Ray, Current state of Fe-Mn-Al-C low density steels, *Progress in Materials Science* 89 (2017) 345-391.
- [18] G. R. Speich, V. A. Demarest, R. L. Miller, Formation of austenite during intercritical annealing of dual-phase steels, *Metallurgical and Materials Transactions A* 12, no. 8 (1981) 1419-1428.
- [19] R. A. Vandermeer, R. A. Masumura, B. B. Rath, Microstructural paths of shape-preserved nucleation and growth transformations, *Acta Metallurgica et Materialia* 39, no. 3 (1991) 383-389.
- [20] Y. Mazaheri, A. Kermanpur, A. Najafizadeh, A. G. Kalashami, Kinetics of Ferrite Recrystallization and Austenite Formation During Intercritical Annealing of the Cold-Rolled Ferrite/Martensite Duplex Structures, *Metallurgical and Materials Transactions A* 47, no. 3 (2016) 1040-1051.
- [21] C. A. Wert, Diffusion coefficient of C in α -iron, *Physical Review* 79, no. 4 (1950) 601-605.

سینتیک تبلور مجدد آستنیت حین آنیل فولاد Fe-Mn-Al-C نورد سرد شده

محمد علی سهرابی زاده، یوسف مظاهری، محسن شیخی

گروه مواد، دانشکده مهندسی، دانشگاه بوعلی سینا، همدان، ایران.

چکیده

رفتار تبلور مجدد آلیاژ Fe-22Mn-10Al-1.4C پس از ۷۵ درصد نورد سرد، در طول عملیات آنیل در دماهای ۷۵۰، ۷۷۰، ۷۹۰، ۸۱۰ و ۸۳۰ درجه سانتی‌گراد مطالعه شد. از الگوی پراش اشعه ایکس و میکروسکوپ نوری جهت مشخصه‌یابی ریزساختاری استفاده شد. از ریزسختی‌سنج ویکرز جهت ارزیابی سینتیک تبلور مجدد در طول آنیل استفاده شد. داده‌های تجربی توسط مدل جانسون-مهل-آورامی-کلموگروف (JMAK) ارزیابی شد. ریزساختار پس از عملیات همگن‌سازی تنها فاز آستنیت همراه با کسر بالایی از دوقلوبی‌ها را نشان داد و استحاله تبدیل آستنیت به مارتنزیت در طول کوئنچ از دمای بالا و تحت کاهش ضخامت زیاد، مشاهده نشد. توان آورامی با افزایش دمای آنیل از ۷۵۰ به ۸۳۰ درجه سانتی‌گراد از ۰/۷۶ به ۰/۴۲ کاهش یافت. مقدار انرژی اکتیواسیون ۱۷۵ کیلوژول بر مول اندازه‌گیری شد که این مقدار کمی بالاتر از انرژی اکتیواسیون نفوذ کربن در آستنیت بود.

واژه‌های کلیدی: فولاد Fe-Mn-Al-C، سینتیک تبلور مجدد، مدل JMAK